PROCEEDINGS OF SCIENCE

PoS(ICRC2025)426

Reconstructing Air-Shower Observables using a Universality-Based Model at the Pierre Auger Observatory

Maximilian Stadelmaier[abc] **for the Pierre Auger Collaboration**[d]
[a] *Istituto Nazionale di Fisica Nucleare INFN, Sezione Milano, Milano, Italy*
[b] *Dipartimento di Fisica, Università degli Studi di Milano, Milano, Italy*
[c] *Institute for Astroparticle Physics, Karlsruhe Institute of Technology KIT, Karlsruhe, Germany*
[d] *Observatorio Pierre Auger, Av. San Martín Norte 304, 5613 Malargüe, Argentina*
Full author list: `https://www.auger.org/archive/authors_icrc_2025.html`

E-mail: `spokespersons@auger.org`

Based on solutions of the cascade equations, the *air-shower universality* is a framework that for all air showers with the same energy, zenith angle, depth of shower maximum, and muon number predicts the same longitudinal, lateral, and energy distributions of electromagnetic shower particles. We employ a universality-based model of shower development that incorporates hadronic particle components to reconstruct observables from extensive air showers produced by ultra-high-energy cosmic rays. The model can estimate key parameters, such as the depth of the shower maximum and the number of muons at the event level. We discuss the performance of the reconstruction algorithm using both air-shower simulations, and preliminary results obtained from the Phase I data of the Pierre Auger Observatory.

39th International Cosmic Ray Conference (ICRC2025)
15 – 24 July 2025
Geneva, Switzerland

ICRC 2025
The Astroparticle Physics Conference
Geneva July 15-24, 2025

1. Introduction

The origin and nature of ultrahigh-energy cosmic rays (UHECRs) is an open problem of modern Astroparticle Physics. In the last decades, the Telescope Array [1] and the Pierre Auger Observatory [2] were established to detect cosmic rays at the highest energies, up to 100 EeV and beyond, and to resolve conflicting results of previous experiments. According to the recent results of the Pierre Auger Observatory, the flux of cosmic rays at the highest energies is composed of an extra-galactic component [3], which is of a mixed-mass composition [4, 5], and which shows spectral features [6] such as a strong suppression of the flux beyond about 50 EeV, for which several different possible explanations have been hypothesized.

Ground-based cosmic ray experiments rely on the detection of the air-shower phenomenon. Air showers occur when very energetic particles enter the Earth's atmosphere, which acts as a calorimeter in which the energy of the primary cosmic ray is converted into cascades of secondary particles that reach up to several kilometers in diameter and comprise approximately 10^9 particles per EeV of the primary energy. They can be detected directly in clear moonless nights by observing the fluorescence light produced by the excitation of nitrogen in the atmosphere, or indirectly by recording the particles that reach the ground. Air-shower profiles, observed as fluorescence light, yield valuable information about the primary cosmic rays. The total fluorescence light emitted is a reliable proxy for the number of particles produced in the air shower, and thus for the energy of the primary; and the development of the air-shower profile through the atmosphere, especially the depth at which it appears the brightest (the *shower maximum*), yields information about the type of the primary particle. Being restricted to nights with optimal atmospheric and light conditions, however, the direct detection of shower profiles is only feasible ~15% of the time. Surface detectors, which are operational up to 100% of the time, do not directly record the air-shower development through the atmosphere, but measure the secondary shower particles that reach the ground in terms of the total particle density as well as the arrival time of the particles. It has been demonstrated that information about the depth of the shower maximum can be inferred empirically from the temporal information of the particles reaching the ground [7]. In this way, information about the shower development is accessible at the highest energies, where the flux of UHECRs is too low to collect a sufficient number of events during the operational time of fluorescence detectors. In this work, we present the depths of the shower maximum of UHECRs recorded by the surface detector of the Pierre Auger Observatory at primary energies above 4 EeV, estimated using a novel method that is based on the established idea of air-shower universality [8–10]. The method makes use of a physically motivated model of the particle densities in air showers and can be extended to extract also other air-shower observables.

2. The Pierre Auger Observatory

The Pierre Auger Observatory is the largest cosmic ray detector in the world. Up to this date it has collected an unprecedented amount of data and exposure during its ~20 years of operation. The observatory is located on the plateau of the Argentinean Pampa Amarilla at an average altitude of 1400 m above sea level. It is equipped with a set of fluorescence detector (FD) telescopes as well as with a $3000\,\mathrm{km}^2$ surface detector (SD) array [11, 12]. Its hybrid detector setup allows for an absolute calibration of the SD using the FD telescopes. The main SD array is comprised of ∼1600 water-Cherenkov detectors (WCDs). The WCDs are each filled with 12 tons of purified water and collect the Cherenkov light emitted by through-going air-shower particles using three photo-multipliers. The signals are digitized and sampled in 25 ns time bins. The detectors are calibrated in terms of VEM, which is the most probable signal of a vertical through-going atmospheric muon [13]. For an overview of the detector operation see [2].

The surface detector is fully efficient to detect cosmic rays above a primary energy of $\lg(E_0/\mathrm{eV}) = 18.5$ (i.e. $E_0 \simeq 3\,\mathrm{EeV}$). Approximately 50 UHECRs are detected each day above full efficiency and within a zenith angle[1] of $\theta \lesssim 60°$ [15], and approximately 25 UHECRs are recorded each day with energies above 4 EeV.

3. Measurement of the Mass Composition of Cosmic Rays

The mass composition of UHECRs cannot be measured directly, but only through proxy observables from air-shower measurements. The atmospheric depth X_max at which the shower reaches its maximum is directly linked to the nuclear mass of the primary cosmic ray [16]. On average, lighter particles of a given energy produce deeper showers, while heavier cosmic rays have shallower development. At the same time, the number of muons in air showers initiated by heavy nuclei is enhanced compared to lighter primaries.

Both the number of muons and the depth of the shower maximum X_max can be accurately measured using the hybrid detector of the Pierre Auger Observatory [4, 17, 18]. Using surface-detector data only, however, this is a challenging task. The surface detector alone has no direct access to information about the air-shower profile, and thus the calorimetric energy deposit as well as the shower development cannot be measured. The energy E_0 of the primary particle and X_max, however, can be estimated from the shower footprint on the ground and from the temporal distribution of the particles in the detectors, respectively [7, 15, 19]. The number of muons, as well, can be estimated from the footprint of the shower at the ground, but, depending on how the total energy estimate is obtained, can be significantly biased with respect to the expectations for different primary particles. An unbiased estimate of the muon number can easily be attained from the shower footprint if an independent energy estimate such as from the FD is utilized.

4. The Universality Shower Model

The model of particle densities used in this work is based on *air-shower universality* [8–10, 20] according to which the expected distribution of particles at the ground can be accurately described as a function of the primary energy E_0 of the UHECR, the depth X_max of the shower maximum, the relative number of muons R_μ, and the event geometry. The model is parametrized using detector-response simulations of the surface detectors of the Pierre Auger Observatory, produced with the $\overline{\text{Off}}\underline{\text{line}}$ software framework using CORSIKA showers generated with the EPOS-LHC model of hadronic interactions [21–23].

---

[1] The Pierre Auger SD is capable of also detecting cosmic rays with arrival directions with $60° < \theta < 80°$, however, due to larger asymmetries arising from the geomagnetic field a special reconstruction technique is applied for such inclined events [14].

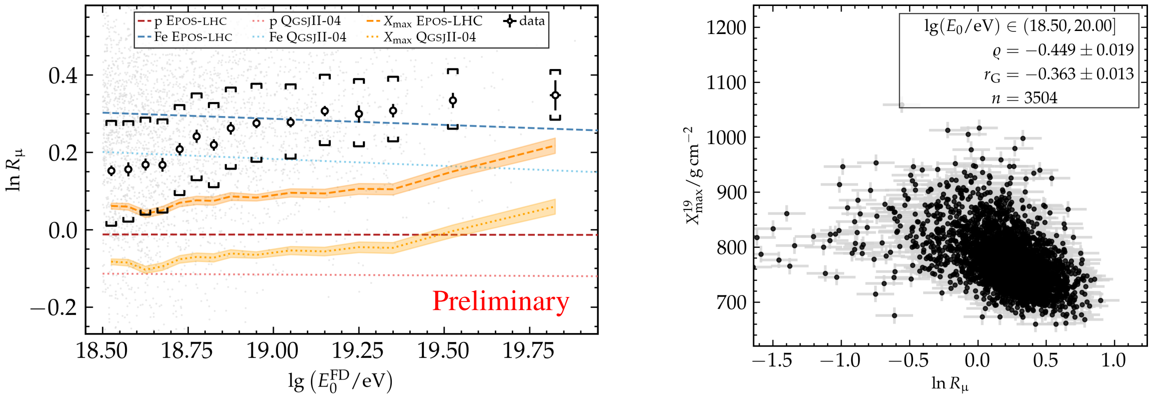

Figure 1: *Left:* The relative muon number as a function of the primary energy measured by the fluorescence detector. The expectations from different hadronic interaction models and primary particles are given as blue and red reference lines. Expectations according to the $X_{\max}$ measurements of the showers are shown in orange. The systematic uncertainties of the estimated number of muons are shown as black brackets around the data points. *Right:* Event-by-event correlation of the depth of the shower maximum and the relative muon number, see Ref. [18] for details.

In the model, the particle content of the shower is divided into different subspecies (components), which are treated separately. In this way, even showers with a large hadronic contribution to the particle content can be described universally. Both the expected lateral and longitudinal development of the shower are parametrized for all particle components as a function of the primary energy, the depth of the shower maximum, and the relative number of muons created in the cascade; additionally, the temporal distribution of the particles at the ground level is parametrized for each component as a function of the depth of the shower maximum and the event geometry. See Ref. [20] for a detailed description of the model itself and the reconstruction mechanism.

5. Golden Hybrid Data: Number of Muons

The number of muons is a quantitative proxy for the hadronic particle production in the shower development and is therefore related to the atomic mass of the initial primary cosmic ray. For different primary particles, the number of muons produced per nucleus does not increase linearly with the primary energy, but approximately $\propto A^{1-\beta}E_0^{\beta}$, with $\beta \simeq 0.95$ [24] and the atomic mass[2] number A. Thus, more muons will be produced in air showers produced by heavy nuclei, as the primary energy is distributed approximately evenly among the nucleons of the primary particle. To accurately estimate the number of shower muons from detector data, an energy estimator that is independent of the shower particle footprint can help to disentangle the apparent dependence of the number of muons with the primary energy. Using the direct fluorescence detector measurements of the shower profile to estimate the primary energy, one can therefore accurately estimate the number of muons produced, given the expected shower footprint of the electromagnetic cascade is known. Therefore the fluorescence detector energy estimate $E_0^{\rm FD}$ is used as an input for the model described

---

[2] For iron nuclei relative to proton nuclei we expect an increase of a factor of $N_{\rm Fe}/N_{\rm p} \approx 56^{1-\beta} = 1.2$ in muons produced.

in Section 4, and the number of muons can be subsequently inferred using a fit. This procedure and the expected performance obtained from simulations are described in detail in Ref. [18].

The number of muons measured with the universality model are shown as a function of the primary energy in Fig. 1 (left) alongside expectations from simulated air showers using the Epos-LHC and QGSJetII-04 [25] models of hadronic interaction. Note that the data selection for the number of muons shown in Fig. 1 is limited to *Golden Hybrid* events where both the fluorescence and surface detector systems were detecting events at the same time; for these events, however, the correlation of the two independent mass-sensitive reconstructed observables yields interesting insights into the broadness of the cosmic-ray beam, see Fig. 1 (right) and Ref. [18]. The logarithm of the muon number is expected to increase linearly with the logarithmic atomic mass number of the primary cosmic ray. The expectations for the number of muons from the measurements of the average $X_{\max}$ are substantially lower than the data. This tension is known as the *muon deficit* or *muon puzzle*, which is present in the data of the Pierre Auger Observatory and other air-shower experiments [17, 26].

6. Surface Detector Data: Depth of the Shower Maximum

The detector time traces (time dependent signals of the water-Cherenkov detectors) are directly related to the shower development. This empirically confirmed connection was used already previously to infer mass-composition information [7], and to estimate the muon production depth [27] using the surface detector data of the Pierre Auger Observatory. For the universality model the detector time traces are parametrized analytically as a function of the shower development, using *time quantiles* and the arrival time of the shower plane front passing through the detector as a reference. The time quantile t_{40}, at which 40% of the (total) signal has been deposited in a detector station, was found to be directly dependent on the distance of the detector to the shower maximum [20]. Using a quasi-spherical shower model, t_{40} is expressed as a function of the shower geometry for each detector station; for details, again see Ref. [20].

Using this model, we fit the time-dependent surface detector data of the Pierre Auger Observatory to estimate the depth of the shower maximum, $X_{\max}$. For this purpose the traces are first normalized (i.e. treated as a PDF) to reduce the effect of both the number of muons and the primary energy on signal size to influence the $X_{\max}$ fit. We thus do not expect the results to be artificially correlated with any other observables. Stations that are far away from the shower axis ($\geq$1800 m) are removed from the fit, since their traces carry little to no information about the depth of the shower maximum, and the model fails to accurately describe the shower data at distances beyond $\simeq$2000 m. The performance of this indirect reconstruction method to estimate $X_{\max}$ was tested both using simulations and Golden Hybrid data. For the latter, the surface detector data was analyzed independently of the fluorescence detector information and the estimated values of $X_{\max}$ were compared for each event. Fig. 2 shows the event-level validation of the method for both simulations and data using directly and indirectly obtained values of $X_{\max}$. Since the data in Fig. 2 span more than one order of magnitude in energy, a constant elongation rate was removed from the data[3] to obtain the $X_{\max}^{19}$ reference values. Although the performance of the universality reconstruction is not *on*

---

[3] $X_{\max}^{19} = X_{\max} - D\ \lg(E_0/10^{19}\,\mathrm{eV})$ using a constant decadal elongation rate, $D \simeq 56\,\mathrm{g/cm^2}$.

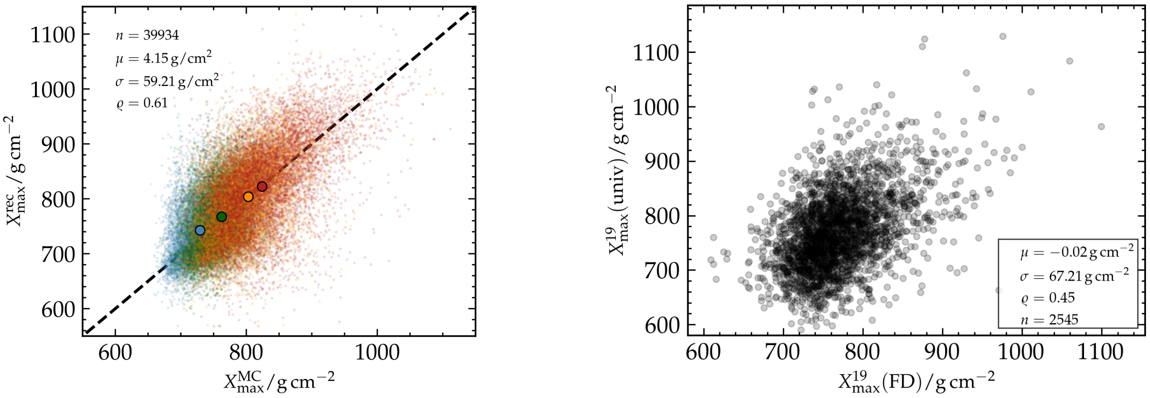

Figure 2: *Left:* True and reconstructed values of X_max for simulated showers above a primary energy of 3 EeV. The number of data points as well as overall mean and width of the residuals $\Delta X_\mathrm{max}^\mathrm{rec}$ are given alongside the Pearson correlation coefficient in the upper left corner. Dot colors correspond to proton, helium, oxygen, and iron. *Right:* Correlation of the estimated (univ) and directly measured (FD) values of the depth of the shower maxima in the Golden Hybrid data set. The moments of the residual distribution as well as the Pearson correlation and the number of events is given in the legend. See the text for details.

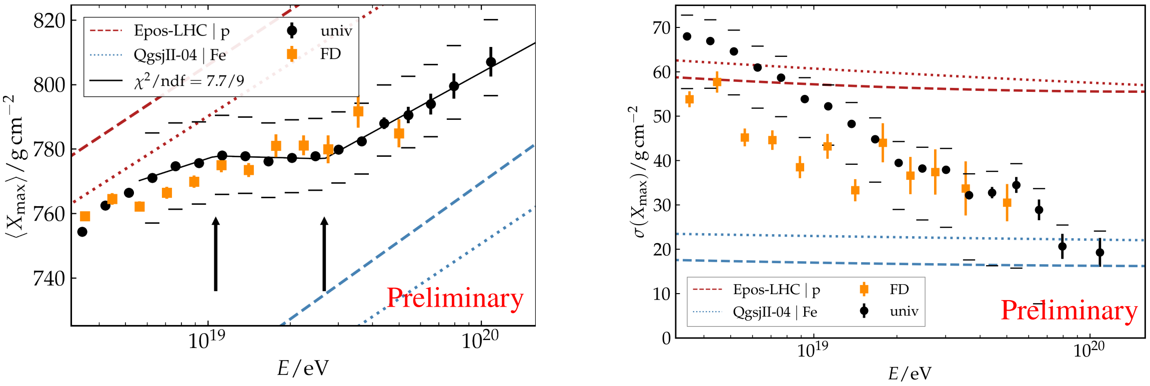

Figure 3: *Left:* Mean X_max as a function of the (SD reconstructed) energy with a broken-line fit. *Right:* Fluctuations of X_max given as the estimated standard deviation of the X_max-distribution, $\sigma(X_\mathrm{max})$, as a function of the primary energy. The black markers denote the mean (or standard-deviation) values from the universality fit, orange markers show the results from direct FD measurements. Black caps stand for the systematic uncertainties. Red and blue dashed and dotted lines indicate the expectation values from simulations using the Epos-LHC and QGSJetII-04 models of hadronic interactions for showers from proton and iron primary particles, respectively.

par with novel machine-learning methods [19, 28–30], we observe a significant correlation for the two data sets. The universality model reconstruction is therefore confirmed to be able to estimate the depth of the shower maximum from the detector time traces.

The X_max as estimated by the universality-model fit applied to the surface detector data of Phase I of the Pierre Auger Observatory are depicted in Fig. 3. The average X_max as a function of the primary energy is monotonically increasing. However, compared to expectations from simulations, the corresponding mean mass $\langle\ln A\rangle$ of ultrahigh-energy cosmic rays is increasing with energy. Furthermore, the mean depth of the shower maximum at high energies evolves with the same elongation rate as expected from single types of primary particles, which implies a somewhat constant mass composition above ≃30 EeV. Where they are available, the results of the universality-model fit (after calibration of the mean) are in reasonable agreement with the data from direct FD measurements in terms of the evolution with primary energy. The first three data points in Fig. 3 (left) are not assigned bars to indicate the systematic uncertainties, because these energies were omitted from the calibration fit, see Section 7.

The fluctuations of $X_{\max}$ as a function of the primary energy were calculated by removing the expected intrinsic precision, as estimated using Monte-Carlo simulations. Above 10 EeV, the qualitative behavior of $\sigma(X_{\max})$ as a function of the primary energy agrees well with the FD data and with expectations from other methods [7, 19, 30]. At lower energies ($E_0 \lesssim 10\,\text{EeV}$), the universality results consistently show larger fluctuations than expected. This could be due to discrepancies of the performance of the method on data with respect to simulations, or possibly due to individual outliers being over-represented. Nevertheless, the behavior of $\sigma(X_{\max})$ as a function of the primary energy implies a heavier and more pure mass composition at the highest energies, and is compatible with a proton-dominated (or helium-dominated) composition around ≃3 EeV, close to the ankle region, for the QGSJetII-04 (or Epos-LHC) model.

Taking a closer look at the evolution of $X_{\max}$ as a function of primary energy above $E_0 = 10^{18.8}\,\text{eV} \simeq 6\,\text{EeV}$, it is immediately clear that the elongation rate appears not to be constant. This has already been studied in depth in Refs. [19, 30], where the elongation rate is best fit with a broken line using two breaks. For comparison, a fit to the data shown in Fig. 3 using only one break yields $\chi^2/\text{ndf} \simeq 45.2/11$ corresponding to $p(\chi^2(\text{ndf})) \simeq 3{\times}10^{-6}$.

7. Systematic Uncertainties and Calibration

Since the results obtained when applying the universality model to data rely heavily on the fluorescence detector either as a source of calibration or direct input, systematic uncertainties are inherited as well. The systematic uncertainties displayed in Figs. 1 and 3 are mostly a direct result of the ≃14% systematic uncertainty of the energy scale of fluorescence detectors and the uncertainty of the $X_{\max}$ calibration. The latter is necessary to correct for an overall difference of the mean $X_{\max}$ provided by raw results of the universality fit and direct measurements; a similar calibration was performed in Refs. [7, 19, 31].

8. Discussion and Summary

The universality-based shower model, described in this work, is an attempt to describe the generalized shower development and use it to reconstruct shower observables. Depending on the input parameters, the model can be used to estimate the number of muons produced in the shower, and/or the depth of the shower maximum on an event level. In general, the reconstructed number of muons is more accurate if an independent energy estimator is used; when trying to reconstruct $X_{\max}$ from the time-dependent signal traces, no event-level fluorescence detector data is required.

The results of the reconstructed shower observables can be used either to infer the details of hadronic interactions in the shower development and maybe introduce new perspectives to mass-composition analyses (see e.g. Ref. [32]), or to qualitatively identify and separate *lighter* or *heavier* events in the data of the Pierre Auger Observatory. Such separated data sets could be used, for example, to reduce background when conducting arrival-direction analyses (see e.g. Ref. [33]).

References

[1] Telescope Array Collaboration, *Nucl. Phys. B Proc. Suppl.* **175** (2008) 221.
[2] Pierre Auger Collaboration, *Nucl. Instrum. Meth. A* **798** (2015) 172 [1502.01323].
[3] Pierre Auger Collaboration, *Science* **357** (2017) 1266–1270.
[4] Pierre Auger Collaboration, *Phys. Rev. D* **90** (2014) 122006 [1409.5083].
[5] Pierre Auger Collaboration, *Phys. Lett. B* **762** (2016) 288 [1609.08567].
[6] Pierre Auger Collaboration, *Phys. Rev. Lett.* **125** (2020) 121106 [2008.06488].
[7] Pierre Auger Collaboration, *Phys. Rev. D* **96** (2017) 122003 [1710.07249].
[8] A.M. Hillas, *J. Phys. G* **8** (1982) 1461.
[9] P. Lipari, *Phys. Rev. D* **79** (2009) 063001 [0809.0190].
[10] F. Nerling, J. Blümer, R. Engel et al., *Astropart. Phys.* **24** (2006) 421 .
[11] Pierre Auger Collaboration, *Nucl. Instrum. Meth. A* **620** (2010) 227 [0907.4282].
[12] Pierre Auger Collaboration, *Nucl. Instrum. Meth. A* **586** (2008) 409 [0712.2832].
[13] Pierre Auger Collaboration, *Nucl. Instrum. Meth. A* **568** (2006) 839 [2102.01656].
[14] Pierre Auger Collaboration, *JCAP* **08** (2014) 019 [1407.3214].
[15] Pierre Auger Collaboration, *J. Instrum.* **15** (2020) 10021 [2007.09035].
[16] J. Matthews, *Astropart. Phys.* **22** (2005) 387.
[17] Pierre Auger Collaboration, *Phys. Rev. D* **91** (2015) 032003 [1408.1421].
[18] Pierre Auger Collaboration, *PoS* **ICRC2023** (2023) 339.
[19] Pierre Auger Collaboration, *Phys. Rev. D* **111** (2025) 022003 [2406.06319].
[20] M. Stadelmaier, R. Engel, M. Roth et al., *Phys. Rev. D* **110** (2024) 023030 [2405.03494].
[21] S. Argiro, S.L.C. Barroso, J. Gonzalez et al., *Nucl. Instrum. Meth. A* **580** (2007) 1485 [0707.1652].
[22] D. Heck, J. Knapp, J. Capdevielle et al., *Report FZKA* **6019** (1998) .
[23] T. Pierog, I. Karpenko, J.M. Katzy et al., *Phys. Rev. C* **92** (2015) 034906 [1306.0121].
[24] J. Matthews, *Astropart. Phys.* **22** (2005) 387.
[25] S. Ostapchenko, *Phys. Rev. D* **83** (2011) 014018 [1010.1869].
[26] J.C. Arteaga Velazquez, *PoS* **ICRC2023** (2023) 466.
[27] Pierre Auger Collaboration, *Eur. Phys. J. Plus* **131** (2016) 301 [1609.02498].
[28] Pierre Auger Collaboration, *PoS* **UHECR2024** (2025) 091.
[29] Pierre Auger Collaboration, *PoS* **ICRC2023** (2023) 371.
[30] Pierre Auger Collaboration, *PRL* (2024) [2406.06315].
[31] Pierre Auger Collaboration, *JINST* **16** (2021) P07019 [2101.02946].
[32] J. Vícha, A. Bakalová, A.L. Müller et al., 2504.11985.
[33] Pierre Auger Collaboration, *PoS* **ICRC2025** (2025) 274.

The Pierre Auger Collaboration

A. Abdul Halim[13], P. Abreu[70], M. Aglietta[53,51], I. Allekotte[1], K. Almeida Cheminant[78,77], A. Almela[7,12], R. Aloisio[44,45], J. Alvarez-Muñiz[76], A. Ambrosone[44], J. Ammerman Yebra[76], G.A. Anastasi[57,46], L. Anchordoqui[83], B. Andrada[7], L. Andrade Dourado[44,45], S. Andringa[70], L. Apollonio[58,48], C. Aramo[49], E. Arnone[62,51], J.C. Arteaga Velázquez[66], P. Assis[70], G. Avila[11], E. Avocone[56,45], A. Bakalova[31], F. Barbato[44,45], A. Bartz Mocellin[82], J.A. Bellido[13], C. Berat[35], M.E. Bertaina[62,51], M. Bianciotto[62,51], P.L. Biermann[a], V. Binet[5], K. Bismark[38,7], T. Bister[77,78], J. Biteau[36,i], J. Blazek[31], J. Blümer[40], M. Boháčová[31], D. Boncioli[56,45], C. Bonifazi[8], L. Bonneau Arbeletche[22], N. Borodai[68], J. Brack[f], P.G. Brichetto Orchera[7,40], F.L. Briechle[41], A. Bueno[75], S. Buitink[15], M. Buscemi[46,57], M. Büsken[38,7], A. Bwembya[77,78], K.S. Caballero-Mora[65], S. Cabana-Freire[76], L. Caccianiga[58,48], F. Campuzano[6], J. Caraça-Valente[82], R. Caruso[57,46], A. Castellina[53,51], F. Catalani[19], G. Cataldi[47], L. Cazon[76], M. Cerda[10], B. Čermáková[40], A. Cermenati[44,45], J.A. Chinellato[22], J. Chudoba[31], L. Chytka[32], R.W. Clay[13], A.C. Cobos Cerutti[6], R. Colalillo[59,49], R. Conceição[70], G. Consolati[48,54], M. Conte[55,47], F. Convenga[44,45], D. Correia dos Santos[27], P.J. Costa[70], C.E. Covault[81], M. Cristinziani[43], C.S. Cruz Sanchez[3], S. Dasso[4,2], K. Daumiller[40], B.R. Dawson[13], R.M. de Almeida[27], E.-T. de Boone[43], B. de Errico[27], J. de Jesús[7], S.J. de Jong[77,78], J.R.T. de Mello Neto[27], I. De Mitri[44,45], J. de Oliveira[18], D. de Oliveira Franco[42], F. de Palma[55,47], V. de Souza[20], E. De Vito[55,47], A. Del Popolo[57,46], O. Deligny[33], N. Denner[31], L. Deval[53,51], A. di Matteo[51], C. Dobrigkeit[22], J.C. D'Olivo[67], L.M. Domingues Mendes[16,70], Q. Dorosti[43], J.C. dos Anjos[16], R.C. dos Anjos[26], J. Ebr[31], F. Ellwanger[40], R. Engel[38,40], I. Epicoco[55,47], M. Erdmann[41], A. Etchegoyen[7,12], C. Evoli[44,45], H. Falcke[77,79,78], G. Farrar[85], A.C. Fauth[22], T. Fehler[43], F. Feldbusch[39], A. Fernandes[70], M. Fernandez[14], B. Fick[84], J.M. Figueira[7], P. Filip[38,7], A. Filipčič[74,73], T. Fitoussi[40], B. Flaggs[87], T. Fodran[77], A. Franco[47], M. Freitas[70], T. Fujii[86,h], A. Fuster[7,12], C. Galea[77], B. García[6], C. Gaudu[37], P.L. Ghia[33], U. Giaccari[47], F. Gobbi[10], F. Gollan[7], G. Golup[1], M. Gómez Berisso[1], P.F. Gómez Vitale[11], J.P. Gongora[11], J.M. González[1], N. González[7], D. Góra[68], A. Gorgi[53,51], M. Gottowik[40], F. Guarino[59,49], G.P. Guedes[23], L. Gülzow[40], S. Hahn[38], P. Hamal[31], M.R. Hampel[7], P. Hansen[3], V.M. Harvey[13], A. Haungs[40], T. Hebbeker[41], C. Hojvat[d], J.R. Hörandel[77,78], P. Horvath[32], M. Hrabovský[32], T. Huege[40,15], A. Insolia[57,46], P.G. Isar[72], M. Ismaiel[77,78], P. Janecek[31], V. Jilek[31], K.-H. Kampert[37], B. Keilhauer[40],p O.W. Kenobi[40,48,58], A. Khakurdikar[77], V.V. Kizakke Covilakam[7,40], H.O. Klages[40], M. Kleifges[39], J. Köhler[40], F. Krieger[41], M. Kubatova[31], N. Kunka[39], B.L. Lago[17], N. Langner[41], N. Leal[7], M.A. Leigui de Oliveira[25], Y. Lema-Capeans[76], A. Letessier-Selvon[34], I. Lhenry-Yvon[33], L. Lopes[70], J.P. Lundquist[73], M. Mallamaci[60,46], D. Mandat[31], P. Mantsch[d], F.M. Mariani[58,48], A.G. Mariazzi[3], I.C. Mariş[14], G. Marsella[60,46], D. Martello[55,47], S. Martinelli[40,7], M.A. Martins[76], H.-J. Mathes[40], J. Matthews[g], G. Matthiae[61,50], E. Mayotte[82], S. Mayotte[82], P.O. Mazur[d], G. Medina-Tanco[67], J. Meinert[37], D. Melo[7], A. Menshikov[39], C. Merx[40], S. Michal[31], M.I. Micheletti[5], L. Miramonti[58,48], M. Mogarkar[68], S. Mollerach[1], F. Montanet[35], L. Morejon[37], K. Mulrey[77,78], R. Mussa[51], W.M. Namasaka[37], S. Negi[31], L. Nellen[67], K. Nguyen[84], G. Nicora[9], M. Niechciol[43], D. Nitz[84], D. Nosek[30], A. Novikov[87], V. Novotny[30], L. Nožka[32], A. Nucita[55,47], L.A. Núñez[29], J. Ochoa[7,40], C. Oliveira[20], L. Östman[31], M. Palatka[31], J. Pallotta[9], S. Panja[31], G. Parente[76], T. Paulsen[37], J. Pawlowsky[37], M. Pech[31], J. Pękala[68], R. Pelayo[64], V. Pelgrims[14], L.A.S. Pereira[24], E.E. Pereira Martins[38,7], C. Pérez Bertolli[7,40], L. Perrone[55,47], S. Petrera[44,45], C. Petrucci[56], T. Pierog[40], M. Pimenta[70], M. Platino[7], B. Pont[77], M. Pourmohammad Shahvar[60,46], P. Privitera[86], C. Priyadarshi[68], M. Prouza[31], K. Pytel[69], S. Querchfeld[37], J. Rautenberg[37], D. Ravignani[7], J.V. Reginatto Akim[22], A. Reuzki[41], J. Ridky[31], F. Riehn[76,j], M. Risse[43], V. Rizi[56,45], E. Rodriguez[7,40], G. Rodriguez Fernandez[50], J. Rodriguez Rojo[11], S. Rossoni[42], M. Roth[40], E. Roulet[1], A.C. Rovero[4], A. Saftoiu[71], M. Saharan[77], F. Salamida[56,45], H. Salazar[63], G. Salina[50], P. Sampathkumar[40], N. San Martin[82], J.D. Sanabria Gomez[29], F. Sánchez[7], E.M. Santos[21], E. Santos[31], F. Sarazin[82], R. Sarmento[70], R. Sato[11], P. Savina[44,45], V. Scherini[55,47], H. Schieler[40], M. Schimassek[33], M. Schimp[37], D. Schmidt[40], O. Scholten[15,b], H. Schoorlemmer[77,78], P. Schovánek[31], F.G. Schröder[87,40], J. Schulte[41], T. Schulz[31], S.J. Sciutto[3], M. Scornavacche[7], A. Sedoski[7], A. Segreto[52,46], S. Sehgal[37], S.U. Shivashankara[73], G. Sigl[42], K. Simkova[15,14], F. Simon[39], L. Skywalker[40,48,58], R. Šmída[86], P. Sommers[e], R. Squartini[10], M. Stadelmaier[40,48,58], S. Stanič[73], J. Stasielak[68], P. Stassi[35], S. Strähnz[38], M. Straub[41], T. Suomijärvi[36], A.D. Supanitsky[7], Z. Svozilikova[31], K. Syrokvas[30], Z. Szadkowski[69], F. Tairli[13], M. Tambone[59,49], A. Tapia[28], C. Taricco[62,51], C. Timmermans[78,77], O. Tkachenko[31], P. Tobiska[31], C.J. Todero Peixoto[19], B. Tomé[70], A. Travaini[10], P. Travnicek[31], M. Tueros[3], M. Unger[40], R. Uzeiroska[37], L. Vaclavek[32], M. Vacula[32], I. Vaiman[44,45], J.F. Valdés Galicia[67], L. Valore[59,49], P. van Dillen[77,78], E. Varela[63], V. Vašíčková[37], A. Vásquez-Ramírez[29], D. Veberič[40], I.D. Vergara Quispe[3], S. Verpoest[87], V. Verzi[50], J. Vicha[31], J. Vink[80], S. Vorobiov[73], J.B. Vuta[31], C. Watanabe[27], A.A. Watson[c], A. Weindl[40], M. Weitz[37], L. Wiencke[82], H. Wilczyński[68], B. Wundheiler[7], B. Yue[37], A. Yushkov[31], E. Zas[76], D. Zavrtanik[73,74], M. Zavrtanik[74,73]

[1] Centro Atómico Bariloche and Instituto Balseiro (CNEA-UNCuyo-CONICET), San Carlos de Bariloche, Argentina
[2] Departamento de Física and Departamento de Ciencias de la Atmósfera y los Océanos, FCEyN, Universidad de Buenos Aires and CONICET, Buenos Aires, Argentina
[3] IFLP, Universidad Nacional de La Plata and CONICET, La Plata, Argentina
[4] Instituto de Astronomía y Física del Espacio (IAFE, CONICET-UBA), Buenos Aires, Argentina
[5] Instituto de Física de Rosario (IFIR) – CONICET/U.N.R. and Facultad de Ciencias Bioquímicas y Farmacéuticas U.N.R., Rosario, Argentina
[6] Instituto de Tecnologías en Detección y Astropartículas (CNEA, CONICET, UNSAM), and Universidad Tecnológica Nacional – Facultad Regional Mendoza (CONICET/CNEA), Mendoza, Argentina
[7] Instituto de Tecnologías en Detección y Astropartículas (CNEA, CONICET, UNSAM), Buenos Aires, Argentina
[8] International Center of Advanced Studies and Instituto de Ciencias Físicas, ECyT-UNSAM and CONICET, Campus Miguelete – San Martín, Buenos Aires, Argentina
[9] Laboratorio Atmósfera – Departamento de Investigaciones en Láseres y sus Aplicaciones – UNIDEF (CITEDEF-CONICET), Argentina
[10] Observatorio Pierre Auger, Malargüe, Argentina
[11] Observatorio Pierre Auger and Comisión Nacional de Energía Atómica, Malargüe, Argentina
[12] Universidad Tecnológica Nacional – Facultad Regional Buenos Aires, Buenos Aires, Argentina
[13] University of Adelaide, Adelaide, S.A., Australia
[14] Université Libre de Bruxelles (ULB), Brussels, Belgium
[15] Vrije Universiteit Brussels, Brussels, Belgium
[16] Centro Brasileiro de Pesquisas Fisicas, Rio de Janeiro, RJ, Brazil
[17] Centro Federal de Educação Tecnológica Celso Suckow da Fonseca, Petropolis, Brazil
[18] Instituto Federal de Educação, Ciência e Tecnologia do Rio de Janeiro (IFRJ), Brazil
[19] Universidade de São Paulo, Escola de Engenharia de Lorena, Lorena, SP, Brazil
[20] Universidade de São Paulo, Instituto de Física de São Carlos, São Carlos, SP, Brazil
[21] Universidade de São Paulo, Instituto de Física, São Paulo, SP, Brazil
[22] Universidade Estadual de Campinas (UNICAMP), IFGW, Campinas, SP, Brazil
[23] Universidade Estadual de Feira de Santana, Feira de Santana, Brazil
[24] Universidade Federal de Campina Grande, Centro de Ciencias e Tecnologia, Campina Grande, Brazil
[25] Universidade Federal do ABC, Santo André, SP, Brazil
[26] Universidade Federal do Paraná, Setor Palotina, Palotina, Brazil
[27] Universidade Federal do Rio de Janeiro, Instituto de Física, Rio de Janeiro, RJ, Brazil
[28] Universidad de Medellín, Medellín, Colombia
[29] Universidad Industrial de Santander, Bucaramanga, Colombia
[30] Charles University, Faculty of Mathematics and Physics, Institute of Particle and Nuclear Physics, Prague, Czech Republic
[31] Institute of Physics of the Czech Academy of Sciences, Prague, Czech Republic
[32] Palacky University, Olomouc, Czech Republic
[33] CNRS/IN2P3, IJCLab, Université Paris-Saclay, Orsay, France
[34] Laboratoire de Physique Nucléaire et de Hautes Energies (LPNHE), Sorbonne Université, Université de Paris, CNRS-IN2P3, Paris, France
[35] Univ. Grenoble Alpes, CNRS, Grenoble Institute of Engineering Univ. Grenoble Alpes, LPSC-IN2P3, 38000 Grenoble, France
[36] Université Paris-Saclay, CNRS/IN2P3, IJCLab, Orsay, France
[37] Bergische Universität Wuppertal, Department of Physics, Wuppertal, Germany
[38] Karlsruhe Institute of Technology (KIT), Institute for Experimental Particle Physics, Karlsruhe, Germany
[39] Karlsruhe Institute of Technology (KIT), Institut für Prozessdatenverarbeitung und Elektronik, Karlsruhe, Germany
[40] Karlsruhe Institute of Technology (KIT), Institute for Astroparticle Physics, Karlsruhe, Germany
[41] RWTH Aachen University, III. Physikalisches Institut A, Aachen, Germany
[42] Universität Hamburg, II. Institut für Theoretische Physik, Hamburg, Germany
[43] Universität Siegen, Department Physik – Experimentelle Teilchenphysik, Siegen, Germany
[44] Gran Sasso Science Institute, L'Aquila, Italy
[45] INFN Laboratori Nazionali del Gran Sasso, Assergi (L'Aquila), Italy
[46] INFN, Sezione di Catania, Catania, Italy
[47] INFN, Sezione di Lecce, Lecce, Italy
[48] INFN, Sezione di Milano, Milano, Italy
[49] INFN, Sezione di Napoli, Napoli, Italy
[50] INFN, Sezione di Roma "Tor Vergata", Roma, Italy
[51] INFN, Sezione di Torino, Torino, Italy

[52] Istituto di Astrofisica Spaziale e Fisica Cosmica di Palermo (INAF), Palermo, Italy
[53] Osservatorio Astrofisico di Torino (INAF), Torino, Italy
[54] Politecnico di Milano, Dipartimento di Scienze e Tecnologie Aerospaziali , Milano, Italy
[55] Università del Salento, Dipartimento di Matematica e Fisica “E. De Giorgi”, Lecce, Italy
[56] Università dell’Aquila, Dipartimento di Scienze Fisiche e Chimiche, L’Aquila, Italy
[57] Università di Catania, Dipartimento di Fisica e Astronomia “Ettore Majorana“, Catania, Italy
[58] Università di Milano, Dipartimento di Fisica, Milano, Italy
[59] Università di Napoli “Federico II”, Dipartimento di Fisica “Ettore Pancini”, Napoli, Italy
[60] Università di Palermo, Dipartimento di Fisica e Chimica ”E. Segrè”, Palermo, Italy
[61] Università di Roma “Tor Vergata”, Dipartimento di Fisica, Roma, Italy
[62] Università Torino, Dipartimento di Fisica, Torino, Italy
[63] Benemérita Universidad Autónoma de Puebla, Puebla, México
[64] Unidad Profesional Interdisciplinaria en Ingeniería y Tecnologías Avanzadas del Instituto Politécnico Nacional (UPIITA-IPN), México, D.F., México
[65] Universidad Autónoma de Chiapas, Tuxtla Gutiérrez, Chiapas, México
[66] Universidad Michoacana de San Nicolás de Hidalgo, Morelia, Michoacán, México
[67] Universidad Nacional Autónoma de México, México, D.F., México
[68] Institute of Nuclear Physics PAN, Krakow, Poland
[69] University of Łódź, Faculty of High-Energy Astrophysics,Łódź, Poland
[70] Laboratório de Instrumentação e Física Experimental de Partículas – LIP and Instituto Superior Técnico – IST, Universidade de Lisboa – UL, Lisboa, Portugal
[71] “Horia Hulubei” National Institute for Physics and Nuclear Engineering, Bucharest-Magurele, Romania
[72] Institute of Space Science, Bucharest-Magurele, Romania
[73] Center for Astrophysics and Cosmology (CAC), University of Nova Gorica, Nova Gorica, Slovenia
[74] Experimental Particle Physics Department, J. Stefan Institute, Ljubljana, Slovenia
[75] Universidad de Granada and C.A.F.P.E., Granada, Spain
[76] Instituto Galego de Física de Altas Enerxías (IGFAE), Universidade de Santiago de Compostela, Santiago de Compostela, Spain
[77] IMAPP, Radboud University Nijmegen, Nijmegen, The Netherlands
[78] Nationaal Instituut voor Kernfysica en Hoge Energie Fysica (NIKHEF), Science Park, Amsterdam, The Netherlands
[79] Stichting Astronomisch Onderzoek in Nederland (ASTRON), Dwingeloo, The Netherlands
[80] Universiteit van Amsterdam, Faculty of Science, Amsterdam, The Netherlands
[81] Case Western Reserve University, Cleveland, OH, USA
[82] Colorado School of Mines, Golden, CO, USA
[83] Department of Physics and Astronomy, Lehman College, City University of New York, Bronx, NY, USA
[84] Michigan Technological University, Houghton, MI, USA
[85] New York University, New York, NY, USA
[86] University of Chicago, Enrico Fermi Institute, Chicago, IL, USA
[87] University of Delaware, Department of Physics and Astronomy, Bartol Research Institute, Newark, DE, USA

---

[a] Max-Planck-Institut für Radioastronomie, Bonn, Germany
[b] also at Kapteyn Institute, University of Groningen, Groningen, The Netherlands
[c] School of Physics and Astronomy, University of Leeds, Leeds, United Kingdom
[d] Fermi National Accelerator Laboratory, Fermilab, Batavia, IL, USA
[e] Pennsylvania State University, University Park, PA, USA
[f] Colorado State University, Fort Collins, CO, USA
[g] Louisiana State University, Baton Rouge, LA, USA
[h] now at Graduate School of Science, Osaka Metropolitan University, Osaka, Japan
[i] Institut universitaire de France (IUF), France
[j] now at Technische Universität Dortmund and Ruhr-Universität Bochum, Dortmund and Bochum, Germany

Acknowledgments

The successful installation, commissioning, and operation of the Pierre Auger Observatory would not have been possible without the strong commitment and effort from the technical and administrative staff in Malargüe. We are very grateful to the following agencies and organizations for financial support:

Argentina – Comisión Nacional de Energía Atómica; Agencia Nacional de Promoción Científica y Tecnológica (ANPCyT); Consejo Nacional de Investigaciones Científicas y Técnicas (CONICET); Gobierno de la Provincia de Mendoza; Municipalidad de Malargüe; NDM Holdings and Valle Las Leñas; in gratitude for their continuing cooperation over land access; Australia – the Australian Research Council; Belgium – Fonds de la Recherche Scientifique (FNRS); Research Foundation Flanders (FWO), Marie Curie Action of the European Union Grant No. 101107047; Brazil – Conselho Nacional de Desenvolvimento Científico e Tecnológico (CNPq); Financiadora de Estudos e Projetos (FINEP); Fundação de Amparo à Pesquisa do Estado de Rio de Janeiro (FAPERJ); São Paulo Research Foundation (FAPESP) Grants No. 2019/10151-2, No. 2010/07359-6 and No. 1999/05404-3; Ministério da Ciência, Tecnologia, Inovações e Comunicações (MCTIC); Czech Republic – GACR 24-13049S, CAS LQ100102401, MEYS LM2023032, CZ.02.1.01/0.0/0.0/16_013/0001402, CZ.02.1.01/0.0/0.0/18_046/0016010 and CZ.02.1.01/0.0/0.0/17_049/0008422 and CZ.02.01.01/00/22_008/0004632; France – Centre de Calcul IN2P3/CNRS; Centre National de la Recherche Scientifique (CNRS); Conseil Régional Ile-de-France; Département Physique Nucléaire et Corpusculaire (PNC-IN2P3/CNRS); Département Sciences de l'Univers (SDU-INSU/CNRS); Institut Lagrange de Paris (ILP) Grant No. LABEX ANR-10-LABX-63 within the Investissements d'Avenir Programme Grant No. ANR-11-IDEX-0004-02; Germany – Bundesministerium für Bildung und Forschung (BMBF); Deutsche Forschungsgemeinschaft (DFG); Finanzministerium Baden-Württemberg; Helmholtz Alliance for Astroparticle Physics (HAP); Helmholtz-Gemeinschaft Deutscher Forschungszentren (HGF); Ministerium für Kultur und Wissenschaft des Landes Nordrhein-Westfalen; Ministerium für Wissenschaft, Forschung und Kunst des Landes Baden-Württemberg; Italy – Istituto Nazionale di Fisica Nucleare (INFN); Istituto Nazionale di Astrofisica (INAF); Ministero dell'Università e della Ricerca (MUR); CETEMPS Center of Excellence; Ministero degli Affari Esteri (MAE), ICSC Centro Nazionale di Ricerca in High Performance Computing, Big Data and Quantum Computing, funded by European Union NextGenerationEU, reference code CN_00000013; México – Consejo Nacional de Ciencia y Tecnología (CONACYT) No. 167733; Universidad Nacional Autónoma de México (UNAM); PAPIIT DGAPA-UNAM; The Netherlands – Ministry of Education, Culture and Science; Netherlands Organisation for Scientific Research (NWO); Dutch national e-infrastructure with the support of SURF Cooperative; Poland – Ministry of Education and Science, grants No. DIR/WK/2018/11 and 2022/WK/12; National Science Centre, grants No. 2016/22/M/ST9/00198, 2016/23/B/ST9/01635, 2020/39/B/ST9/01398, and 2022/45/B/ST9/02163; Portugal – Portuguese national funds and FEDER funds within Programa Operacional Factores de Competitividade through Fundação para a Ciência e a Tecnologia (COMPETE); Romania – Ministry of Research, Innovation and Digitization, CNCS-UEFISCDI, contract no. 30N/2023 under Romanian National Core Program LAPLAS VII, grant no. PN 23 21 01 02 and project number PN-III-P1-1.1-TE-2021-0924/TE57/2022, within PNCDI III; Slovenia – Slovenian Research Agency, grants P1-0031, P1-0385, I0-0033, N1-0111; Spain – Ministerio de Ciencia e Innovación/Agencia Estatal de Investigación (PID2019-105544GB-I00, PID2022-140510NB-I00 and RYC2019-027017-I), Xunta de Galicia (CIGUS Network of Research Centers, Consolidación 2021 GRC GI-2033, ED431C-2021/22 and ED431F-2022/15), Junta de Andalucía (SOMM17/6104/UGR and P18-FR-4314), and the European Union (Marie Sklodowska-Curie 101065027 and ERDF); USA – Department of Energy, Contracts No. DE-AC02-07CH11359, No. DE-FR02-04ER41300, No. DE-FG02-99ER41107 and No. DE-SC0011689; National Science Foundation, Grant No. 0450696, and NSF-2013199; The Grainger Foundation; Marie Curie-IRSES/EPLANET; European Particle Physics Latin American Network; and UNESCO.